

Time-resolved investigation of coherent LO-phonon relaxation in III-V semiconductors

Fabrice Vallée

*Laboratoire d'Optique Quantique du Centre National de la Recherche Scientifique, Ecole Polytechnique,
91128 Palaiseau Cedex, France*

(Received 12 August 1993)

Relaxation of coherent LO phonons is investigated in InP, GaAs, and GaP by use of an infrared time-resolved coherent anti-Stokes Raman-scattering technique. Measurements were performed as a function of crystal temperature in the range 6–320 K. The measured LO-phonon dephasing times are about four-times longer in InP than in GaAs. This difference is attributed to the closing of the cubic combination relaxation channel which dominates the decay in GaAs but is energetically forbidden in InP. In this compound, as in GaP, both a less efficient combination relaxation channel and the overtone decay route where the initial phonon splits into two isoenergetic longitudinal-acoustic phonons significantly contribute to the LO-phonon decay.

I. INTRODUCTION

Interaction of optical phonons with their environment is one of the key parameters in most of the physical properties of semiconductors. Optical-phonon energy and phase relaxation has thus been widely investigated in semiconductors with a special emphasis on polar compounds where the LO phonons mediate energy exchanges between the hot electrons and the lattice.^{1–5} Spontaneous Raman spectroscopy has been an important source of information allowing the determination of the dominant optical-phonon relaxation mechanisms in various semiconductors.^{5–11} In technologically important polar III-V compounds such as GaAs and InP, there is, however, a large discrepancy between the reported Raman linewidths precluding an unambiguous qualitative and quantitative determination of the LO-phonon broadening mechanisms. In these semiconductors additional information is clearly required to understand LO-phonon anharmonic interactions with the other degrees of freedom of the lattice.

Time-resolved techniques constitute important and reliable tools for the investigation of vibrational relaxation dynamics in dense systems.^{12,13} They have been widely exploited in liquids and in molecular crystals but only scarcely in semiconductors.^{13,14} The LO-phonon population relaxation time (T_1) has been measured for a few temperatures in GaAs and $\text{Al}_x\text{Ga}_{1-x}\text{As}$ alloys using time-resolved incoherent Raman spectroscopy to monitor the temporal evolution of the nonequilibrium incoherent phonon population created by cascade hot-electron relaxation.^{14,15} The problem of coherent LO-phonon decay has recently been addressed in semiconductors by use of femtosecond transient reflectivity¹⁶ and of the picosecond time-resolved coherent anti-Stokes Raman-scattering (CARS) technique.¹³ This last technique gives only access to the temporal evolution of the envelope of the excited LO-phonon wave packet but has the advantage of a very high sensitivity and of a high accuracy. In time-resolved CARS measurements, a coherent phonon population is first created in the bulk of the sample by coherent Raman

scattering of two synchronized picosecond pulses ω_L and ω_S whose frequency difference matches the frequency ω_0 of the investigated phonon, $\omega_L - \omega_S = \omega_0$. The excitation pulses lie in the transparency region of the sample limiting the modifications of the phonon environment due to carrier photoexcitation. The temporal evolution of the coherence of the excitation is followed by coherent anti-Stokes Raman scattering at $\omega_p + \omega_0$ of a time-delayed picosecond probe pulse ω_p yielding access to the phonon dephasing time (T_2).¹⁷ LO phonons are associated to an electromagnetic field and their coupling with the laser beams occurs through both their mechanical and electromagnetic component. However, the general description developed for nonpolar excitation can be applied using an effective Raman tensor as long as a quantitative description of the absolute value of the measured intensity is not required.^{18–20}

In semiconductors, time-resolved CARS has first been used to investigate LO-phonon dephasing in visible gap compounds (GaP and ZnSe) (Ref. 20) and recently in infrared gap compounds (GaAs).²¹ In this last investigation, an infrared version of the time-resolved CARS technique has been used to determine the LO-phonon dephasing time in GaAs for crystal temperature ranging from 6 to 215 K. In this temperature range, coherent decay has been shown to be dominated by an intraband population relaxation channel similar to the optical-phonon decay route in group-IV semiconductors.^{5,21}

To further test the relevance of the proposed relaxation mechanism in GaAs we have performed temperature-dependent measurements of the LO-phonon dephasing in the range 215–320 K by use of an improved version of our infrared time-resolved CARS setup.²¹ The same technique has been applied to study LO-phonon dephasing in InP where the modifications of the phonon band structure compared to GaAs are expected to deeply alter the LO-phonon relaxation channels. To our knowledge, this constitutes the first accurate determination of the LO-phonon relaxation time in InP where the linewidths inferred by our dephasing time measurements are much smaller than those previously reported using spontaneous

Raman scattering. Additional measurements performed in GaP are also reported and compared to the results of Kuhl and Bron²⁰ in order to check a possible sample-dependent contribution to the measured dephasing rate and to test the proposed relaxation mechanism in InP.

II. LO-PHONON RELAXATION

Phonon dephasing in crystals is a consequence of both the intrinsic anharmonicity of the lattice and of spatial modulation of its order. In good-quality samples, processes induced by spatial disorder, such as scattering by impurities and defects, play a minor role and the finite phonon dephasing time takes its origin in phonon-phonon interactions caused by anharmonicity of the crystal potential. Anharmonic phonon relaxation and energy renormalization have been investigated by many authors^{22–24} and only a brief description of the relevant results will be given here. The lowest-order anharmonic term in the crystal potential is the third-order anharmonicity $H^{(3)}$,

$$H^{(3)} = \sum_{\substack{i_1, i_2, i_3 \\ k_1, k_2, k_3}} V_{i_1 i_2 i_3}^{(3)}(k_1, k_2, k_3) A_{i_1 k_1} A_{i_2 k_2} A_{i_3 k_3}. \quad (1)$$

where $n(\omega)$ is the statistical occupation number of the phonon with frequency ω and ω_{iq} is the energy of the phonon belonging to the i branch with wave vector q . The preceding expression ensures wave-vector and energy conservation while symmetry conservation is included in the anharmonic-coupling coefficients. The first term corresponds to a down-conversion process where the initial ω_0 phonon with wave vector $k \sim 0$ decays into two lower-energy phonons, ω_i and ω_j , with opposite wave vector. The second term describes phonon up-conversion where the initial excitation is scattered by a thermal phonon (i, q) into a phonon of higher energy (j, q) . In zinc-blende crystal there is no phonon of higher energy than the zone center LO phonons and hence no up-conversion mechanism is allowed. To the lowest anharmonic order, relaxation thus occurs by splitting of the initial phonon into two lower-energy phonons such that $\omega_{iq} + \omega_{j-q} = \omega_{LO}$. This can be realized either for $i=j$ (overtone channel), or for $i \neq j$ (combination channel), depending on the phonon band structure of the investigated material. Following the approximation introduced by Klemens to carry out analytic calculations,²⁵ the overtone channel has been frequently invoked as an efficient relaxation channel for the optical phonons. As pointed out by several authors,^{5,10} although frequently energetically possible, this decay route is less likely than the combination channels because of the stringent limitations imposed by energy and wave-vector conservation.

If we assume that the anharmonic coefficients are

$A_{ik} = (b_{ik} + b_{i-k}^\dagger)$ is the vibration amplitude of the phonon belonging to the i branch with wave vector k and (b_{ik}^\dagger, b_{ik}) the phonon creation and annihilation operators.

$V_{i_1 i_2 i_3}^{(3)}(k_1, k_2, k_3)$ is a cubic anharmonic coupling coefficient. For LO phonons, the longitudinal electric field associated with the mechanical motion renormalizes the anharmonic coefficients which include contributions from both the mechanical and electro-optical anharmonicity.¹⁹ It has been recently shown that this duality in the anharmonic interactions of a polar mode plays an important role in the damping dispersion of the transverse mode (polariton mode).¹⁹ Separation of the two contributions is, however, not essential for the undispersed longitudinal mode and the problem can be treated as for a nonpolar phonon, by considering effective coupling coefficients.

Using the standard procedure,²⁴ one can show that for weak interactions, anharmonicity leads to a Lorentzian broadening of the phonon lines with a linewidth proportional to the imaginary part of the phonon self-energy. The broadening, $\Gamma_0^{(3)}$ [full width at half maximum (FWHM)], of the ω_0 phonon in the center of the Brillouin zone resulting from cubic anharmonicity is given by

$$\Gamma_0^{(3)} = \frac{36\pi}{\hbar^2} \sum_{i,j,q} |V_{oij}^{(3)}(0, q, -q)|^2 \{ [1 + n(\omega_{iq}) + n(\omega_{j-q})] \delta(\omega_0 - \omega_{iq} - \omega_{j-q}) + 2[n(\omega_{iq}) - n(\omega_{jq})] \delta(\omega_0 + \omega_{iq} - \omega_{jq}) \}, \quad (2)$$

wave-vector independent and that the dispersion of the final phonons is small, the LO-phonon linewidth due to cubic processes in zinc-blende crystal can be written

$$\Gamma_0^{(3)}(\omega_{LO}) = \sum_{i,j} \Gamma_{ij}(\omega_{LO}) [1 + n(\omega_i) + n(\omega_j)] \times d_{\omega_i + \omega_j}(\omega_{LO}), \quad (3)$$

where $d_{\omega_i + \omega_j}(\omega)$ is the density of states of the $\omega_i + \omega_j$ two-phonon band at the frequency ω and at $k=0$. Γ_{ij} are average coupling coefficients. The efficiency of the interaction processes is proportional to the density of state of the final two-phonon band and, hence, relaxation channels involving zone-edge phonons are expected to give the dominant contributions. Discrimination between the different allowed channels can be realized through their different behavior with crystal temperature. Neglecting the temperature dependence of the coupling coefficients, cubic processes depend on temperature through linear combinations of the occupation numbers of the final phonons (2), leading to a characteristic linear variation of the relaxation rate at high temperature. In contrast, higher-order mechanisms involved nonlinear combinations of the occupation numbers resulting in a nonlinear temperature dependence of the relaxation rate.²⁶ The temperature variation of the phonon broadening is, thus, the signature allowing the determination of both the nature of the dominant interaction mechanisms and of the energy of the involved phonons.

The theoretical investigation summarized above has been carried out in the frequency domain but the results can be easily extended to the time domain. For the Lorentzian broadening of a phonon line obtained with the hypothesis of a weak anharmonic perturbation, the phonon dephasing time T_2 and the phonon linewidth Γ_0 (in cm^{-1}) are related by¹⁷

$$\Gamma_0 = 1/\pi c T_2. \quad (4)$$

For a weak broadening, time-resolved experiments are expected to be more accurate especially for crystals with a transparency domain limited to the infrared. Furthermore, time-resolved CARS being a bulk technique, the measured dephasing times are free from any surface effects.⁹

III. EXPERIMENTAL SYSTEM

Creation and probing of coherent phonons in the bulk of the crystal with the time-resolved CARS technique requires picosecond pulses in the transparency region of the sample, i.e., in the near infrared for GaAs ($E_{\text{gap}} \sim 1.51$ eV at 77 K) and InP ($E_{\text{gap}} \sim 1.41$ eV at 77 K). These pulses are produced by a modified version of the passively mode-locked cavity dumped Nd:glass laser system already described and utilized for visible CARS experiments.²⁷ This system generates 5-ps pulses at a wavelength of $1.054\text{-}\mu\text{m}$. After amplification to 2 mJ, the initial pulse is split into three parts to create the ω_L , ω_S , and ω_p beams. The first one ($< 10 \mu\text{J}$), is passed through a variable delay and is used as the probe beam (ω_p) while the second one ($< 30 \mu\text{J}$) is utilized as one of the excitation beams (ω_L). The second excitation pulse at the frequency $\omega_S = \omega_L - \omega_{\text{LO}}$ is created by frequency shifting the third part by stimulated Raman scattering in a liquid whose Stokes shift is close to the LO-phonon frequency of the investigated semiconductor [CHBr₂Cl for GaAs ($\omega_{\text{LO}} = 295 \text{ cm}^{-1}$ at 77 K), SnCl₄ for InP ($\omega_{\text{LO}} = 350 \text{ cm}^{-1}$ at 77 K), and GeCl₄ for GaP ($\omega_{\text{LO}} = 405 \text{ cm}^{-1}$ at 77 K)]. After frequency filtering, the energy of the ω_S beam is of the order of 2 μJ . The linear polarization of the three beams is adjusted (ω_S and ω_p are vertically polarized and ω_L is horizontally polarized) and they are slightly focused into the sample using a noncolinear geometry to satisfy the phase-matching requirement. The focal spot diameter is measured to be 390 μm for the ω_L and ω_p beam and 300 μm for the ω_S beam. The focusing and the energy of the incoming pulses have been limited in order to avoid any perturbation from carriers photoexcited by two-photon absorption²⁸ and by residual one-photon absorption from impurities.²⁹ For each sample the energy of the pulses has been set by checking the independence of the measured decay on the beam intensities. This energy is lower in InP than in GaAs, probably because of its lower band gap. No intensity-dependent effect has been observed in GaP up to the damage threshold because of its lower two-photon absorption which involves only indirect gap transitions for the photon energy of our laser (1.177 eV).³⁰ The anti-Stokes signal is detected by an S1 photomultiplier after spatial and spectral

filtering. For the geometry used in our experiment, the anti-Stokes signal is linearly polarized (horizontal) allowing additional polarization selection.

The GaAs sample is a high-quality semi-insulating crystal (residual concentration $< 10^{15}$ electrons/ cm^3) with a thickness of 320 μm . The InP sample is 290 μm thick and has a residual electron concentration of $8 \times 10^{15} \text{ cm}^{-3}$. The thickness of the samples has been chosen to permit a sufficient interaction length without degrading too much the temporal resolution.²¹ For a large focal spot, multiple reflections of the excitation beams inside a sample of intermediate thickness result in a repetitive excitation of the phonon mode that severely limits the temporal resolution, the signal decay being observed over several orders of magnitude. In the thin GaAs and InP samples, the resolution of the system has been measured to be 1.2 ps and has been found to be limited by the thickness of the samples. Measurements were also performed in a thick GaP crystal (1 mm) with a tighter focusing of the incoming beams. In these conditions the multiple reflections are spatially separated and the intrinsic temporal resolution of our system for infrared CARS has been measured under nonresonant conditions ($\omega_L - \omega_S = 350 \text{ cm}^{-1}$) to be better than 1 ps. The three samples have (100) surfaces and were oriented with their crystallographic axis in the horizontal and vertical direction. In zinc-blende crystals, this geometry, with the excitation pulses cross polarized, realizes the optimum coupling of the excitation and probing beams with the LO phonons. Because of the polariton effect at a small wave vector¹⁹ and of the chosen beam polarization and crystal orientation, the influence of the TO phonons on the measured signal is negligible. The samples were glued on the cold finger of a nitrogen- or helium-cooled cryostat allowing temperatures between 6 and 320 K.

IV. EXPERIMENTAL RESULTS

The observed CARS signal measured in InP is plotted on a logarithmic scale as a function of probe delay in Fig. 1, for two crystal temperatures (78 and 300 K). The temporal shape is similar to the one measured in GaAs.²¹ The initial transient observed for probe delays shorter than 5 ps is attributed to the two-photon resonant electronic nonlinear response of the crystal. Due to the sub-picosecond carrier relaxation, no free carrier response occurs on a picosecond time scale and the observed signal closely follows the system response function (dashed line in Fig. 1). For probe delay longer than 5 ps, an exponential decrease of the coherent signal is observed over more than two orders of magnitude. The slope of the decay measures the LO-phonon dephasing time $T_2/2 = 22 \pm 2$ ps at 78 K and $T_2/2 = 7.6 \pm 0.6$ ps at 300 K, much longer than in GaAs for the same temperatures (6.4 and 2.1 ps, respectively). The low-temperature dephasing time (40 ± 7 ps at 6 K) is more than four times longer than in GaAs [9.2 ps at 6 K (Ref. 21)] indicating a different origin of the phonon relaxation. The measured temperature dependence of the LO-phonon dephasing rate, $2/T_2$, in InP is shown in Fig. 2 for temperatures ranging from 6–300 K.

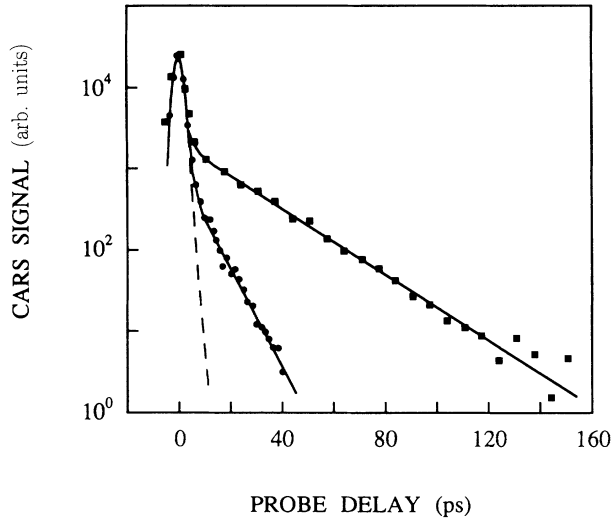


FIG. 1. Coherent anti-Stokes signal from the LO phonon in InP, plotted on a logarithmic scale as a function of probe delay in picoseconds. The crystal temperature is 78 K (squares) and 300 K (circles). The slope of the decay for long probe delay ($t_D > 5$ ps) measures the LO-phonon dephasing time: $T_2/2 = 22 \pm 2$ and 7.6 ± 0.6 ps, respectively. The dashed line is the system response function.

Similar measurements were performed in GaAs in the temperature range 77–320 K. At liquid-nitrogen temperature the results are identical to those previously reported, and we have centered our investigation on the temperature range 200–320 K not covered in Ref. 21. The dephasing rates measured in the present investigation are

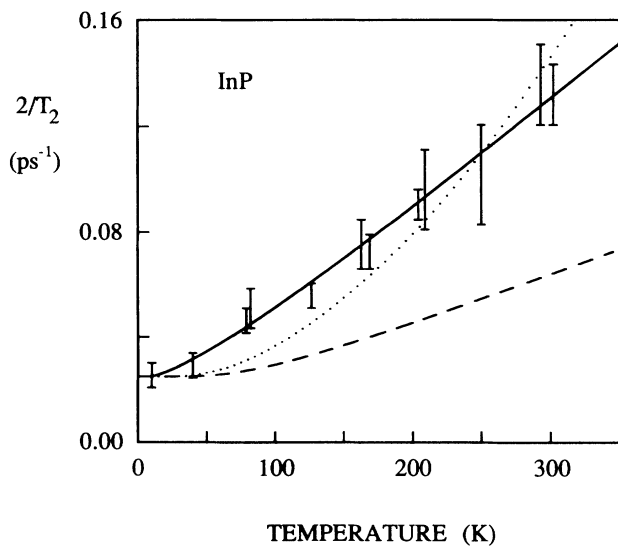


FIG. 2. Measured dephasing rate, $\Gamma_{LO} = 2/T_2$, of the LO phonon in InP as a function of crystal temperature. The solid line is calculated for almost identical contributions from the cubic overtone channel and a cubic combination channel (7) (see text). The dashed line corresponds to a contribution from only the cubic overtone channel (6) and the dotted line to contributions from the third- and fourth-order overtone channels [(6) and (8)].

plotted together with those of Ref. 21 in Fig. 3. Although the wave vectors of the LO phonons accessed in CARS experiments are much smaller than in techniques based on spontaneous Raman backscattering, the results can be compared since in both of these experiments the phonon wave vector is small compared to the Brillouin zone and, hence, the modification of the anharmonic interactions and of the phonon energy is negligible. At 300 K the measured dephasing time, $T_2/2$, is 2.1 ± 0.2 ps corresponding to a FWHM linewidth of 2.55 ± 0.25 cm^{-1} in good agreement with recent Raman data (2.6 cm^{-1}).³¹ This confirms the Lorentzian broadening of the LO-phonon line. Taking into account experimental accuracy, the measured dephasing times are identical to the lifetimes measured for a few temperatures¹⁴ indicating a negligible contribution from pure dephasing effects. The LO-phonon dephasing times recently measured using femtosecond transient reflectivity in GaAs are also comparable.¹⁶

The CARS signal measured in GaP is shown in Fig. 4 for a crystal temperature of 300 K. The phase decay of the LO phonon is followed over five orders of magnitude in spite of the use of nonresonant infrared pulses (the photon energy is about half the indirect gap energy). The measured dephasing time (6.8 ± 0.6 ps at 300 K) is comparable to that determined by Kuhl and Bron using a time-resolved visible CARS technique²⁰ and three times longer than in GaAs. The results are identical over the whole temperature range studied as shown in Fig. 5. Some of the linewidths measured using spontaneous Raman scattering^{20,11} are also reported for comparison.

The importance of limiting the incoming beam intensity is illustrated in Fig. 6 where we have plotted the CARS signal measured in InP at room temperature for a

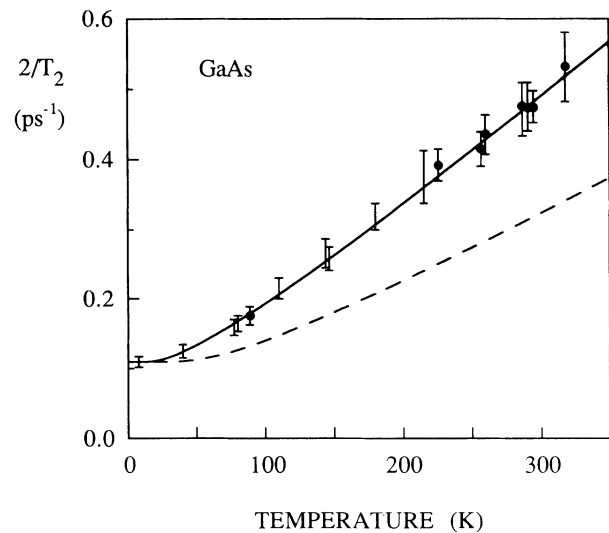


FIG. 3. Measured dephasing rate, $\Gamma_{LO} = 2/T_2$, of the LO phonon in GaAs as a function of crystal temperature. The bars with a solid circle correspond to the present investigation in a thin crystal. The other data (bars) are from Ref. 21. The solid line is calculated taking into account only the cubic intraband combination channel (5) (see text). The dashed line corresponds to a contribution from only the cubic overtone channel (6).

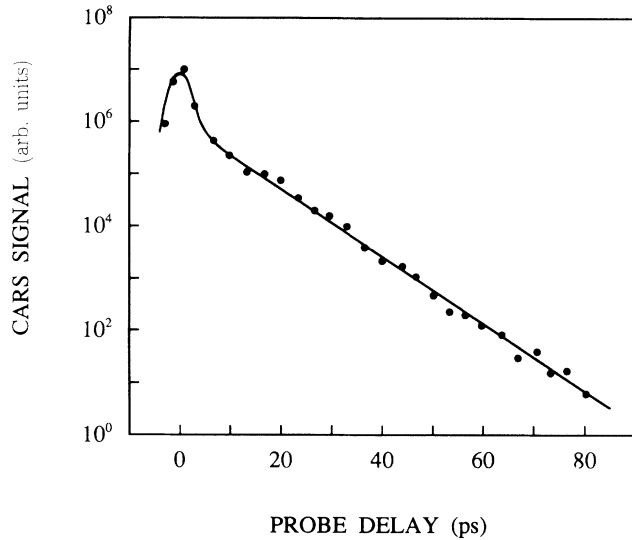


FIG. 4. Coherent anti-Stokes signal from the LO phonon in GaP as a function of probe delay. The crystal temperature is 300 K. The measured dephasing time is $T_2/2 = 6.8 \pm 0.6$ ps.

ω_L pulse energy of 15 μJ (upper curve) and of 1 μJ (lower curve). For the higher laser energy the temporal shape of the signal is deeply modified and the decay is no more exponential for a probe delay shorter than 25 ps. For a longer delay, the signal recovers its original exponential decay with the same characteristic time as measured at low energy. Because of the very low average power used

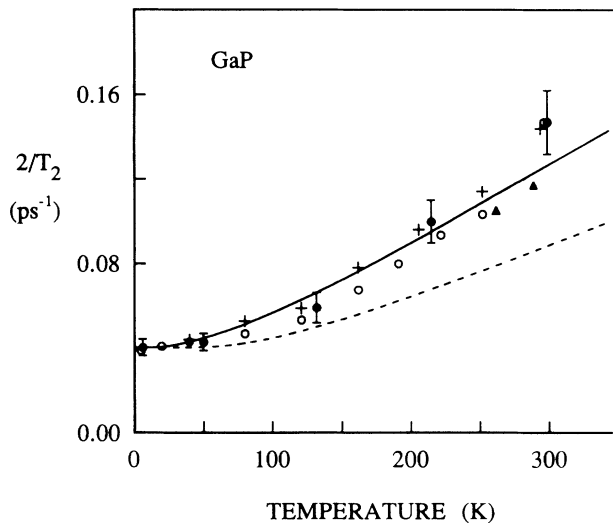


FIG. 5. Measured dephasing rate, $\Gamma_{\text{LO}} = 2/T_2$, of the LO phonon in GaP as a function of crystal temperature. The solid circles correspond to the present investigation. The open circles and the crosses correspond, respectively, to the time-resolved CARS and to the spontaneous Raman measurements of Kuhl and Bron (Ref. 20). The solid triangles are from the high-temperature Raman linewidth measured by Bairamov *et al.* (Ref. 11). The solid line is calculated for contributions from the cubic overtone channel and the cubic combination channel (7) (see text) while the dashed line is calculated for only the cubic overtone channel (6).

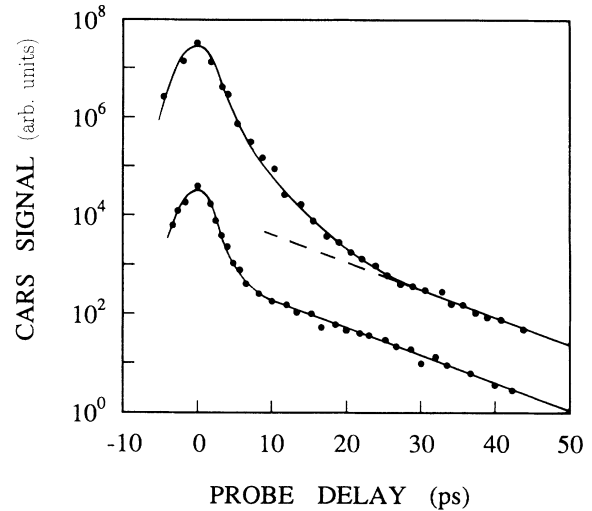


FIG. 6. Temporal dependence of the coherent anti-Stokes signal from the LO phonon in InP at 300 K for a ω_L pulse energy of 15 μJ (upper curve) and 1 μJ (lower curve). The upper curve has been up-shifted for clarity and the actual maximum of the signal (at $t_D = 0$) varies linearly with the intensity of the ω_L pulse.

in our experiment ($< 20 \mu\text{W}$) thermal effects are unlikely and the origin of the deviation lies in the high peak power of the laser. A similar nonexponential decay of the CARS signal has previously been reported in GaP at low temperature and has been attributed to excitation of a nonequilibrium phonon state appearing at large phonon densities.³² The origin of the deviation is different in our experiment since we have checked that the shape of the signal is independent of the coherent phonon density by varying the ω_S beam energy for both a high intensity and a low intensity of the ω_L beam. The temporal shape of the signal is also independent of the probe pulse intensity and its maximum amplitude varies linearly with the energy of each of the incoming beams. We suggest that the effect originates from free carrier photoexcitation by two-photon absorption of the ω_L pulse (the effect of the low intensity ω_S beam is much smaller). On the base of the measured picosecond nonlinear absorption in GaAs,³³ the density of the photoexcited electron-hole plasma is estimated to be of the order of $5 \times 10^{17} \text{ cm}^{-3}$ for a laser pulse energy of 15 μJ . This density is sufficient to significantly accelerate the LO-phonon dephasing due to its coupling with the collective mode of the plasma.^{28,34-36} The photoexcited plasma can be considered as static on the time scale of our experiment since it almost thermalizes during the duration of the pulses and its decay by recombination and transverse diffusion occurs on a much longer time scale (a few hundred picoseconds³⁷). The decrease of the plasma density is thus not the origin of the recovery of the original dephasing time for long probe delays. We believe that the observed behavior results from the radial spatial inhomogeneity of the created plasma which induces a radial variation (with plasma density) of the effective LO-phonon dephasing rate over the excited zone.³⁶ For a sufficiently long time delay only phonons with the longest decay time (i.e., the

decay measured at low intensity), on the edges of the focal spot, are observed. The origin of the deviation has been confirmed by increasing the probe beam focusing so that the photoexcited plasma can be considered as homogeneous over the probed zone. In these conditions at high laser energy, an exponential decay of the CARS signal is measured with a dephasing time much shorter than at low laser energy.³⁸

V. DISCUSSION

The difference in the absolute value of the measured decay rate of the LO phonons in GaAs, InP, and GaP can be qualitatively understood on the base of the third-order anharmonic-interaction model discussed in Sec. II. In GaAs, it has been shown that the dominant relaxation channel in the temperature range 6–215 K is intraband decay into a transverse-acoustic (TA) phonon ($\nu_{TA} \sim 60 \text{ cm}^{-1}$) and a LO phonon of opposite wave vector in the vicinity of the L critical point of the Brillouin zone.²¹ The corresponding temperature dependence of the damping rate Γ_{LO} is given by (2):

$$\Gamma_{LO}^{\text{GaAs}} = \gamma_0 [1 + n(\nu_{TA}) + n(\nu_{LO})], \quad (5)$$

where γ_0 is an effective anharmonic constant. If only one mechanism is considered, the measured low-temperature relaxation rate fixes the only free parameter γ_0 (the occupation numbers being negligible for $T < 10 \text{ K}$). Using this expression with the value of the anharmonic coefficient determined in Ref. 21 ($\gamma_0 = 0.11 \text{ ps}^{-1}$), the experimental data measured in the range 6–320 K are very well reproduced (solid line in Fig. 3) yielding further evidence for the dominance of the intraband combination relaxation channel in GaAs.

The experimental and calculated phonon dispersion curves^{39,40} show that two other three-phonon down-conversion processes satisfy energy and wave-vector conservation for LO-phonon relaxation in GaAs.²¹ These are LO phonon splitting into a TA phonon ($\nu_{TA} \sim 80 \text{ cm}^{-1}$) and a longitudinal-acoustic (LA) phonon ($\nu_{LA} \sim 215 \text{ cm}^{-1}$) near the K and X points of the Brillouin zone and splitting into two LA phonons with half the LO-phonon energy and opposite wave vector along the Σ , Λ , and Δ directions of the Brillouin zone (cubic overtone process). Addition of one of these decay channels to the previous one leads to a slower temperature increase of the relaxation rate and worsens the fit of Fig. 3. However, within the experimental errors, the experimental data can still be fairly reproduced by introduction of small contributions from the (TA+LA) process (up to 30% of the total relaxation rate at $T=0$) or from the overtone process (up to 10% of the total relaxation rate at $T=0$). As previously discussed,²¹ the low efficiency of the overtone channel is due to both the symmetry selection and to the small density of the final states in a region of large dispersion of the LA mode, far from the edges of the Brillouin zone. In fact, inspection of the one-phonon density of states³⁹ shows that the LO-phonon energy corresponds to a minimum in the density of states of the acoustical overtones.

As GaAs, InP, and GaP have a zinc-blende structure

and consequently comparable phonon band structures with a weaker dispersion of the LO-phonon mode due to the higher mass difference of the constituent atoms.^{40–43} Intraband relaxation of zone center LO phonons into zone-edge optical phonons is consequently not allowed by energy and wave-vector conservation. We believe that this is the origin of the large increase of the LO-phonon relaxation time in InP and GaP compared to GaAs. In both of these semiconductors the overtone channel is the only three-phonon interaction mechanism involving zone-edge phonons [around the X and K points of the Brillouin zone in InP (Fig. 7) and the W and L points in GaP]. The overtone process is thus more probable than in GaAs and is expected to significantly contribute to the LO-phonon decay. Although the amplitude of the anharmonic interactions can also vary, the dominance of the combination channel in GaAs and the larger relaxation time measured in InP and GaP show that the overtone channel has a lower efficiency than the combination channels. This is attributed to the fact that the Γ_{15} component of the two-phonon spectrum, satisfying symmetry conservation for relaxation of the LO mode, is mainly due to combination bands rather than to overtone modes.^{44,45} The symmetry selection thus renders the overtone channel less likely than the combination channels.

The role of the cubic overtone channel in InP and GaP can be tested by comparing the predicted and measured temperature dependence of the decay rate. This dependence is given by (2):

$$\Gamma_{LO}^{\text{ov}} = \gamma_0 [1 + 2n(\omega_{LO}/2)], \quad (6)$$

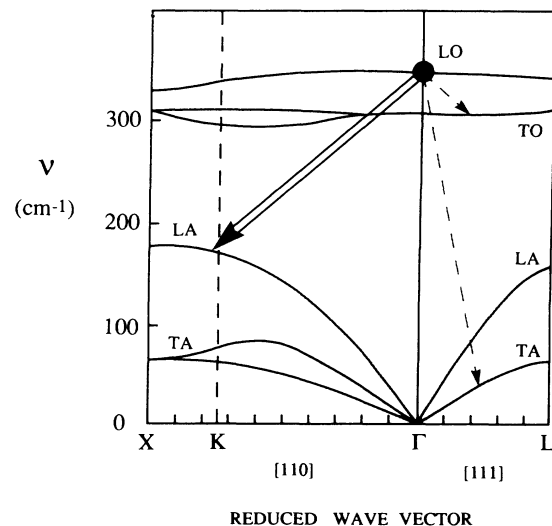


FIG. 7. Phonon dispersion curve of InP in the L and X directions of the Brillouin zone (Ref. 43). The double arrow schematizes the relaxation of the zone center LO phonons into two isoenergetic LA phonons of opposite wave vector (cubic overtone channel) close to the K point. The dashed arrows correspond to the cubic combination relaxation channel into small wave-vector TO and TA phonons along the Γ - L direction. Note that this process is possible along all the directions of the Brillouin zone and that LA phonons can also contribute.

where, as pointed out above, γ_0 is the low temperature relaxation rate. Using this expression for InP, with $\gamma_0=0.025 \text{ ps}^{-1}$, the calculated temperature dependence is too slow to describe the experimental results (dashed line in Fig. 2) demonstrating the intervention of an additional phase relaxation process. This second process might take its origin in both the intrinsic anharmonic properties of the crystal and in the modification of the carrier environment by thermal activation. Note that dephasing introduced by spatial disorder is essentially temperature independent and is thus not likely to contribute.

The linearity of the temperature dependence of the dephasing rate in InP for temperature higher than 50 K suggests that, as in GaAs, anharmonic relaxation is dominated by cubic processes. In the preceding discussion, we have neglected three-phonon processes involving phonons with low density of states (i.e., far from the edges of the Brillouin zone). Taking into account energy and wave-vector conservation, the measured and calculated band structures⁴¹⁻⁴³ show that zone center LO phonons can be annihilated into small wave-vector TO and TA (or LA) phonons at different points of the Brillouin zone with $\nu_{\text{TA}}=30 \text{ cm}^{-1}$ (Fig. 7). This process is similar to the dominant decay route in GaAs but is less probable because of the weaker density of states of the final phonons. Taking into account this second process, the total relaxation rate can be written

$$\Gamma_{\text{LO}}^{\text{InP}} = (\gamma_0 - \gamma)[1 + 2n(\omega_{\text{LO}}/2)] + \gamma[1 + n(\nu_{\text{TA}}) + n(\nu_{\text{TO}})], \quad (7)$$

where γ is a fitting parameter. The calculated dependence is shown by the solid line in Fig. 2 and gives a good description of the experimental results for comparable contributions of the two processes ($\gamma_0=0.025 \text{ ps}^{-1}$ and $\gamma=0.013 \text{ ps}^{-1}$). Note that such an agreement cannot be obtained without inclusion of the overtone process.

Although a good description of the measurements is obtained including only three-particle interactions, higher-order anharmonic mechanisms might also contribute to the LO-phonon decay. Fourth-order processes have frequently been invoked as efficient relaxation channels in semiconductors. Due to the multiplicity of the possible decay route no channel can be *a priori* singled out and a simplified model based on a generalization of the cubic overtone channel has been used.^{6,10} This fourth-order overtone channel corresponds to LO phonon splitting into three LA phonons of the same energy ($\omega_{\text{LA}}=\omega_{\text{LO}}/3$) and the temperature dependence of its contribution, $\Gamma_{\text{LO}}^{(4)}$, to the LO-phonon relaxation rate is given by⁶

$$\Gamma_{\text{LO}}^{(4)} = \gamma^{(4)} \{ 1 + 3n(\omega_{\text{LO}}/3) + 3[n(\omega_{\text{LO}}/3)]^2 \}. \quad (8)$$

In contrast to cubic relaxation channels, the resulting decay rate exhibits a nonlinear temperature dependence characteristic of a higher-order process. Adding this contribution to expression (6) for the cubic overtone process gives only a poor description of the results (dotted line in Fig. 2) indicating a small influence of the fourth-order mechanisms.

For the long dephasing times measured in InP and GaP, small modifications of the residual carrier density by thermal activation might also influence the LO-phonon phase decay. This effect is, however, expected to increase linearly with electron concentration³⁵ and thus nonlinearly with temperature⁴⁶ in contrast with the measured linear temperature dependence of Γ_{LO} for temperature higher than 50 K. This linearity and the good reproduction of the experimental results by expression (7) thus suggest that plasma effects and higher-order anharmonicity play a minor role and that cubic overtone and combination relaxation channels dominate the decay.

In GaP, using spontaneous Raman technique and visible time-resolved CARS, it has been shown that the low-temperature LO-phonon relaxation is dominated by the cubic overtone channel.^{11,20} The LO-phonon dephasing rates we measured for a few temperatures are comparable to the previous determinations indicating a small influence of crystal impurities and defects. The relevance of the overtone process at low temperature is confirmed by comparison of the measured data with expression (6) (dashed line in Fig. 5). The deviation observed for temperature higher than 150 K indicates that, as in InP, an additional relaxation mechanism has to be included. The results can be fairly reproduced by addition of a cubic combination mechanism (TO+TA) identical to the one invoked in InP, with, because of energy conservation, $\nu_{\text{TA}}=50 \text{ cm}^{-1}$. Using expression (7) we obtain the full line in Fig. 5 with $\gamma_0=0.04 \text{ ps}^{-1}$ and $\gamma=0.014 \text{ ps}^{-1}$, corresponding to a dominant contribution from the overtone channel. The temperature increase of the dephasing rate is, however, less linear than in InP and is also compatible with an additional contribution from a fourth-order process. Including both the third- and fourth-order overtone mechanisms [expressions (6) and (8)], a good description of the results is obtained but with a large fourth-order coefficient ($\gamma^{(4)} \sim 0.01 \text{ ps}^{-1}$) compared to the cubic one ($\gamma^{(3)} \sim 0.03 \text{ ps}^{-1}$). The agreement thus seems to be fortuitous and, as in InP, cubic processes are likely to dominate. Thermally activated carriers might also play a role close to room temperature as suggested by the smaller relaxation rate deduced from the high-resolution Raman data of Bairamov *et al.*¹¹

VI. CONCLUSION

LO-phonon dephasing has been investigated in three III-V semiconductors (InP, GaAs, and GaP) by use of an infrared time-resolved CARS technique. Measurements were performed as a function of crystal temperature from 6 K to room temperature and the results are interpreted in terms of anharmonic interaction of the LO phonon with its phonon environment. The relative simplicity of the phonon band structure of the zinc-blende compounds results in a limited number of energetically allowed relaxation channels which can be discriminated through their behavior with crystal temperature. Up to room temperature, the LO-phonon relaxation in bulk GaAs is dominated by intraband decay into a TA phonon and a LO phonon (combination channel) in the vicinity of the *L* critical point of the Brillouin zone while the contribution of the

decay channel into two LA phonons (cubic overtone channel) is found to be negligible.²¹

The measured LO-phonon dephasing times are much larger in InP and in GaP than in GaAs (about four and three times larger, respectively). This difference is attributed to the fact that in contrast to GaAs no combination relaxation channel involving zone-edge phonons is allowed by energy and wave-vector conservation. The intraband combination channel prevailing in GaAs is thus ineffective in InP and GaP and the cubic overtone channel significantly contributes to the LO-phonon relaxation. Moreover, in both of these semiconductors, the overtone channel is more probable than in GaAs since it involves LA phonons of high density of states, close to the edge of the Brillouin zone. The major role played by the combination channel in GaAs and the smaller decay rate measured in InP and GaP indicate a weak anharmonic coupling of the LO phonons with the acoustic overtones, probably because of symmetry selection.

The temperature dependence of the measured dephasing rate demonstrates that although associated with a large density of final states, the overtone channel does not dominate the LO-phonon decay in InP. A good description of the results is obtained by including almost identical contributions from the cubic overtone channel and from a cubic combination channel where the LO phonon splits into a pair of small wave-vector phonons (TO+TA). This last process is, in essence, identical to

the dominant LO-phonon decay route in GaAs and to the optical-phonon relaxation channel in group-IV semiconductors.⁵ In InP (and in GaP) it, however, involves final phonons close to the center of the Brillouin zone and is thus less probable than in GaAs because of the low density of the final states. The measured decay rate in GaP can be reproduced on the base of the same model with, however, a larger contribution of the overtone channel, confirming the central role played by the combination channel, optical-phonon+TA phonon, in III-V semiconductors.

The sensitivity of the measured LO-phonon dynamics to the presence of a photoexcited electron-hole plasma has also been demonstrated in InP. Coherent investigations of the LO-phonon-plasmon hybrid modes together with incoherent lifetime measurements could bring new insights into the dynamical properties of the collective plasma mode in semiconductors.

ACKNOWLEDGMENTS

I gratefully acknowledge C. Flytzanis for his critical reading of the manuscript and F. Bogani for his participation in the early stage of this experiment and for helpful discussions. I also wish to thank D. Paget and J. Walker for kindly providing the GaP and GaAs crystals and Sumitomo Electric Industries, Semiconductor Division, Japan, for providing the InP sample.

-
- ¹L. Reggiani, in *Hot Electron Transport in Semiconductors*, edited by L. Reggiani (Springer-Verlag, Berlin, 1985), p. 7.
- ²S. A. Lyon, *J. Lumin.* **35**, 121 (1986).
- ³W. Pötz and P. Kocevar, *Phys. Rev. B* **28**, 7040 (1983).
- ⁴J. C. Vaissiere, J. P. Nougier, M. Fadel, L. Hlou, and P. Kocevar, *Phys. Rev. B* **46**, 1308 (1992).
- ⁵J. Menendez and M. Cardona, *Phys. Rev. B* **29**, 2051 (1984).
- ⁶M. Balkanski, R. F. Wallis, and E. Haro, *Phys. Rev. B* **28**, 1928 (1983).
- ⁷R. K. Chang, J. M. Ralston, and D. E. Keating, in *Light Scattering Spectra of Solids*, edited by G. B. Wright (Springer-Verlag, Berlin, 1969), p. 369.
- ⁸B. Jusserand and J. Sapriel, *Phys. Rev. B* **24**, 7194 (1981).
- ⁹P. J. Evans and S. Ushioda, *Phys. Rev. B* **9**, 1638 (1974).
- ¹⁰B. Kh. Bairamov, Yu. E. Kitaev, V. K. Negoduiko, and Z. M. Khashkhovzhev, *Fiz. Tverd. Tela (Leningrad)* **16**, 2036 (1974) [*Sov. Phys. Solid State* **16**, 1323 (1975)].
- ¹¹B. Kh. Bairamov, D. A. Parshin, V. V. Toporov and Sh. B. Ubaidullaev, *Pis'ma Zh. Tekh. Fiz.* **5**, 1116 (1979) [*Sov. Tech. Phys. Lett.* **5**, 467 (1979)].
- ¹²R. R. Alfano and S. L. Shapiro, *Phys. Rev. Lett.* **26**, 1247 (1971); A. Seilmeier and W. Kaiser, in *Ultrashort Laser Pulses and Applications*, edited by W. Kaiser (Springer-Verlag, Berlin, 1988), p. 279.
- ¹³A. Laubereau, in *Semiconductors Probed by Ultrafast Laser Spectroscopy*, edited by R. R. Alfano (Academic, New York, 1984), p. 275.
- ¹⁴J. A. Kash and J. C. Tsang, in *Light Scattering in Solids VI*, edited by M. Cardona and G. Guntherodt (Springer-Verlag, Berlin, 1991), p. 423.
- ¹⁵D. von der Linde, J. Kuhl, and H. Klingenberg, *Phys. Rev. Lett.* **44**, 1505 (1980).
- ¹⁶W. A. Kütt, W. Albrecht, and H. Kurz, *IEEE J. Quantum Electron.* **28**, 2434 (1992).
- ¹⁷A. Laubereau and W. Kaiser, *Rev. Mod. Phys.* **50**, 607 (1978).
- ¹⁸W. Hayes and R. Loudon, *Scattering of Light by Crystals* (Wiley, New York, 1978).
- ¹⁹F. Vallée and C. Flytzanis, *Phys. Rev. B* **46**, 13 799 (1992).
- ²⁰J. Kuhl and W. E. Bron, *Solid State Commun.* **49**, 935 (1984); W. E. Bron, J. Kuhl, and B. K. Rhee, *Phys. Rev. B* **34**, 6961 (1986).
- ²¹F. Vallée and F. Bogani, *Phys. Rev. B* **43**, 12 049 (1991).
- ²²R. A. Cowley, *Rep. Prog. Phys.* **31**, 123 (1968).
- ²³I. P. Ipatova, A. A. Maradudin, and R. F. Wallis, *Phys. Rev.* **155**, 882 (1967).
- ²⁴S. Califano, V. Schettino, and N. Neto, in *Lattice Dynamics of Molecular Crystals*, Lecture Notes in Chemistry (Springer-Verlag, Berlin, 1981).
- ²⁵P. G. Klemens, *Phys. Rev.* **148**, 845 (1966).
- ²⁶S. Califano and V. Schettino, *Int. Rev. Phys. Chem.* **7**, 19 (1988).
- ²⁷F. Vallée, *Chem. Phys. Lett.* **175**, 377 (1990).
- ²⁸R. S. Turtelli and A. R. B. de Castro, *Phys. Status Solidi B* **93**, 811 (1979).
- ²⁹K. T. Tsen, D. A. Abramo, and R. Bray, *Phys. Rev. B* **26**, 4770 (1982).
- ³⁰J. H. Bechtel and W. L. Smith, *Phys. Rev. B* **13**, 3515 (1976).
- ³¹J. A. Kash, S. S. Jha, and J. C. Tsang, *Phys. Rev. Lett.* **58**, 1869 (1987).
- ³²W. E. Bron, T. Juhasz, and S. Mehta, *Phys. Rev. Lett.* **62**, 1655 (1989).
- ³³B. Bosacchi, J. S. Bessey, and F. C. Jain, *J. Appl. Phys.* **49**,

- 4609 (1978).
- ³⁴G. Abstreiter, M. Cardona, and A. Pinczuk, in *Light Scattering in Solids IV*, edited by M. Cardona and G. Guntherodt (Springer-Verlag, Berlin, 1984), p. 5.
- ³⁵F. Vallée, F. Bogani, and C. Flytzanis, in *Time Resolved Vibrational Spectroscopy*, edited by H. Takahashi (Springer-Verlag, Berlin, 1992), p. 272.
- ³⁶F. Bogani and F. Vallée, in *Ultrafast Processes in Spectroscopy*, edited by A. Laubereau and A. Selmeier (IOP, Bristol, 1992), p. 203.
- ³⁷K. T. Tsen, G. Halama, O. F. Sankey, S. C. Y. Tsen, and H. Morkoc, *Phys. Rev. B* **40**, 8103 (1989).
- ³⁸F. Vallée (unpublished).
- ³⁹D. Strauch and B. Dorner, *J. Phys. Condens. Matter* **2**, 1457 (1990).
- ⁴⁰K. Kunk, M. Balkanski, and N. A. Nusimovici, *Phys. Status Solidi B* **72**, 229 (1975).
- ⁴¹M. Vandevyver and P. Plumelle, *J. Phys. Chem. Solids* **38**, 765 (1977).
- ⁴²E. Bedel, G. Landa, R. Carles, J. P. Redoulès, and J. B. Renucci, *J. Phys. C* **19**, 1471 (1986).
- ⁴³M. S. Kushwaha and S. S. Kushwaha, *Can. J. Phys.* **58**, 351 (1980).
- ⁴⁴R. Trohmer and M. Cardona, *Phys. Rev. B* **17**, 1865 (1978).
- ⁴⁵M. Lax, V. Narayahurti, R. C. Fulton, R. Bray, K. T. Tsen, and K. Wan, in *Phonon Scattering in Condensed Matter*, edited by W. Eisenmenger, K. Labmann, and S. Döttinger (Springer-Verlag, Berlin, 1984), p. 133.
- ⁴⁶G. E. Stillman, C. M. Wolfe, and J. O. Dimmock, in *Semiconductors and Semimetals*, edited by R. K. Willardson and A. C. Beer (Academic, New York, 1977), Vol. 12, p. 169.